Cell Biology

# C-terminal tagging, transmembrane domain hydrophobicity, and an ER retention motif influence the secretory trafficking of the inner nuclear membrane protein emerin

Reviewed Preprint
v2 • July 16, 2025
Revised by authors

Reviewed Preprint
v1 • March 27, 2025

**Jessica Mella, Regan Volk, Balyn Zaro, Abigail Buchwalter**

Cardiovascular Research Institute, University of California, San Francisco, San Francisco, United States • Department of Pharmaceutical Chemistry, University of California, San Francisco, San Francisco, United States • Department of Physiology, University of California, San Francisco, San Francisco, United States



**eLife Assessment**

This study presents a **valuable** finding on the delivery of a nuclear envelop protein to lysosomes and the impact of C-terminal tagging on its traffic. The authors provide **solid** evidence for the potential artifacts introduced by large terminal tags, particularly in the context of membrane protein localization and stability.

https://doi.org/10.7554/eLife.105937.2.sa3

## Abstract

The inner nuclear membrane (INM), a subdomain of the endoplasmic reticulum (ER), sequesters hundreds of transmembrane proteins within the nucleus. We previously found that one INM protein, emerin, can evade the INM by secretory transport to the lysosome, where it is degraded. In this work, we used targeted mutagenesis to identify intrinsic sequences that promote or inhibit emerin's secretory trafficking. By manipulating these sequences across several tag and expression level combinations, we now find that emerin's localization is sensitive to C-terminal GFP tagging. While emerin's long, hydrophobic C-terminal transmembrane domain facilitates trafficking to the lysosome, extending its lumenal terminus with a GFP tag biases the protein toward this pathway. In contrast, we identify a conserved ER retention sequence that stabilizes N- and C-terminally tagged emerin by limiting its lysosomal flux. These findings underscore long- standing concerns about tagging artifacts and reveal novel determinants of tail-anchored INM protein targeting.

## Introduction

Tail-anchored proteins of the inner nuclear membrane (INM) are a unique class of transmembrane proteins with poorly understood biosynthesis, targeting, and degradation. The INM is a specialized extension of the endoplasmic reticulum (ER) membrane, the major site of membrane protein synthesis. Shortly after translation, tail-anchored proteins are embedded by their C-terminal transmembrane domains into the ER[1]. Unlike cytoplasmic tail-anchored proteins, which rapidly traffic out of the ER toward their target membranes, INM proteins must remain in the ER long enough to diffuse through the nuclear pore complex (NPC) and be retained by binding to nuclear structures[2,3]. This process repeats each time the nuclear envelope reforms at the end of mitosis[4]. INM proteins thus spend considerable time in the ER, but how they interact with the ER's secretory or proteostatic functions is unclear.

Our previous work identified emerin (EMD) as a short-lived INM protein in C2C12 mouse myoblasts[5]. While investigating how emerin is degraded, we found that C-terminally GFP-tagged emerin travels by vesicular transport to the Golgi, plasma membrane (PM), and then lysosome during ER stress[5]– an itinerary that closely tracks with the path taken by cargoes of the rapid ER stress-induced export (RESET) pathway[6]. This unexpected secretory trafficking was prevented by the removal of EMD-GFP's N-terminal LEM domain, suggesting that this domain played a role in stress-induced lysosomal degradation. We hypothesized that the INM might dynamically respond to ER stress by shunting emerin through the secretory pathway to the lysosome. However, we now find that N-terminally GFP-tagged emerin traffics at a lower rate than C- terminally tagged emerin, and find no conclusive evidence that untagged emerin traffics to the lysosome. We also show that the secretory trafficking of tagged emerin depends on its unusually hydrophobic transmembrane domain (TMD). In isolation, the TMDs of both emerin and the related tail-anchored protein LAP2β readily traffic to the PM, but trafficking of the full-length tagged proteins is limited by a conserved RXR-type ER retention motif. Our experiments indicate that emerin's trafficking is artifactually expedited by C-terminal GFP tagging. However, these studies identify sequence elements that target emerin to the contiguous nuclear envelope/endoplasmic reticulum (NE/ER) network and highlight the interdependence between protein biogenesis, topology, and localization.

## Results

After our initial discovery, we aimed to understand the mechanism of emerin's secretory trafficking and its conservation across species, cell types, and expression levels. As our earlier experiments used C2C12 mouse myoblasts, we first tested whether EMD-GFP trafficking is conserved in human cells. We stably expressed tet-inducible mouse and human GFP fusions in human osteosarcoma (U2OS) cells. When treated with the lysosome blocking agent bafilomycin A1 (BafA1), we found that U2OS cells, unlike C2C12 myoblasts[5], do not rely on ER stress to initiate secretory trafficking of EMD-GFP. Instead, BafA1 alone caused EMD-GFP to accumulate in lysosomal puncta. We used this high secretory flux to differentiate between emerin constructs that could and could not traffic (**Figure 1A**). Consistent with our C2C12 findings, we verified that WT EMD-GFP could traffic to the lysosome of U2OS cells, while a construct lacking the N-terminal LEM domain (βLEM, **Figure 1B**) could not. Our constructs were tagged with a C-terminal/lumenal GFP, which allowed us to quantify the proportion of EMD-GFP in the secretory pathway using cell surface antibody labeling and flow cytometry (**Figure 1C,D**). We calculated the trafficking level of each construct by dividing the surface anti-GFP antibody signal by the total EMD-GFP fluorescence. In line with our microscopy experiments, the anti-GFP antibody did not detect any βLEM construct at the PM of U2OS cells, while the WT EMD-GFP PM signal was always above background (**Figure 1E**).

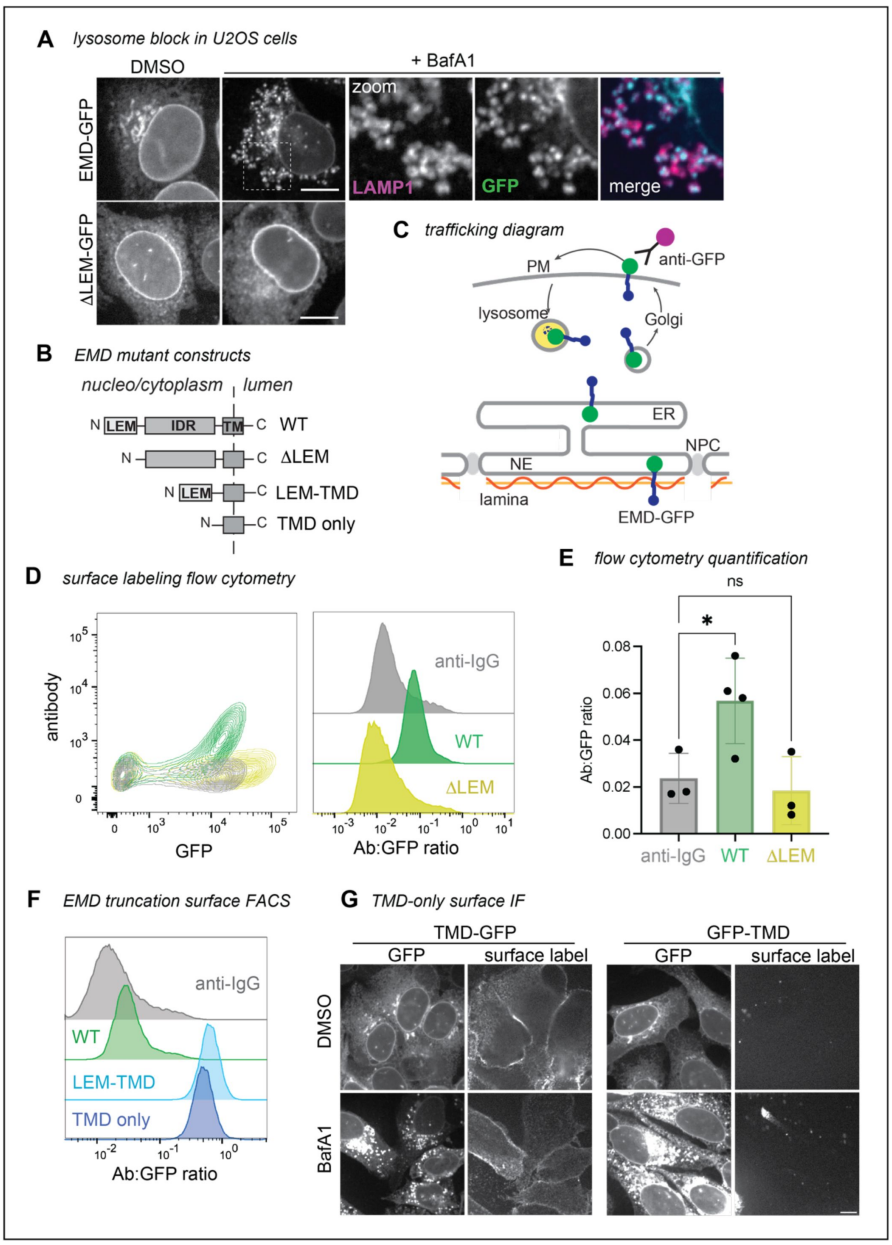


## Figure 1.

### EMD βLEM does not traffic in U2OS cells, while the TMD alone does.

**A)** U2OS cells expressing mouse EMD-GFP and βLEM-GFP were induced with 1 ug/mL doxycycline for 24 hours, treated with 100nM lysosome blocking agent Bafilomycin A1 (BafA1) overnight, and fixed and stained for lysosome marker Lamp1. Scale bar, 10 um.
**B)** Summary of EMD domains and truncation mutants.
**C)** EMD enriches at the INM by binding to the nuclear lamina, or exits the ER into the secretory pathway. Before reaching the lysosome, EMD transiently accesses the cell surface where lumenal GFP is exposed to anti-GFP antibody.
**D)** Example FACS plot of mouse WT vs βLEM surface labeling; fluorescent anti-IgG secondary antibody included as background control. Antibody signal is divided by total GFP+ signal to yield histograms on the right.
**E)** Quantification of the antibody:GFP ratio from 4 independent experiments, with error bars representing SD. * indicates adjusted P-value = 0.0451 by one-way ANOVA with Šídák's multiple comparisons test.
**F)** U2OS cells expressing mouse TMD-GFP (lumenal tag) or GFP-TMD (cytosolic tag) were treated overnight with BafA1, then fixed and stained with an anti-GFP antibody.
**G)** Example surface labeling FACS histogram of U2OS cells expressing WT, LEM-TMD-GFP, or TMD-GFP.

## Emerin's hydrophobic transmembrane domain is necessary and sufficient for trafficking of EMD-GFP

We further leveraged this U2OS system to examine how emerin's protein sequence facilitates trafficking. Emerin contains three major domains: an N-terminal LEM domain that interacts with the chromatin crosslinker BANF1/BAF, an intrinsically disordered region (IDR) that binds the nuclear lamina, and a C-terminal transmembrane domain (TMD)[7] (**Figure 1B**). We tested each domain's ability to traffic through the secretory pathway with a series of domain truncation experiments. Having established that removing the LEM domain abolished emerin's ability to traffic, we next deleted the disordered region between the LEM domain and the transmembrane domain (TMD). This construct (termed LEM-TMD) accumulated at the PM 10-fold more than the WT protein, indicating that the TMD, LEM domain, or both together are sufficient for trafficking (**Figure 1F**). To distinguish between these possibilities, we tested whether emerin's TMD alone can travel to the PM. We removed all but the TMD alpha helix and its surrounding 26 residues (mEMD 212-259), which we found to be required for membrane insertion of the truncated construct (not shown), and appended this TMD-only construct to either the C- or N-terminus of eGFP. Both TMD-GFP and GFP-TMD localized prominently to the ER and PM, and both were evident in the lysosome after BafA1 treatment (**Figure 1F-G**). These experiments reveal that emerin's TMD alone can traffic to the lysosome, regardless of GFP tag orientation.

We wondered what properties of emerin's TMD mediate its secretion. Tail-anchored proteins can sort via their TMDs along the secretory pathway[8–10]; long and hydrophobic sequences partition to the thicker, more hydrophobic membranes of the late secretory organelles[11] (Figure S2B-C), while tail-anchored proteins with shorter, less hydrophobic TMDs preferentially remain in the ER. We noticed that emerin's TMD is particularly hydrophobic among other NE/ER transmembrane domains (Figure S2A-B), which led us to predict that emerin's TMD is required for its exit from the ER. To test this, we replaced emerin's TMD with that of cytochrome B5, a model ER protein with a modestly hydrophobic TMD[12]. This substitution ablated trafficking through the secretory pathway (**Figure 2A-B**), indicating that emerin's TMD is indeed necessary for trafficking. We tested whether this depended on the hydrophobic content of the alpha helix by sequentially mutating its aromatic residues to alanine. We divided the TMD into N- and C-terminal halves, mutating three aromatic amino acids in each half (**Figure 2C**). The N-terminal TMD mutant was slightly less hydrophobic and had a greater effect on secretory trafficking than the C-terminal mutant (**Figure 2D-E**). Combining the N- and C-terminal mutations additively reduced the surface ratio of EMD-GFP. While these mutations decreased the overall protein expression (Figure S2E), they did not affect the protein's topology (Figure S2F), confirming that the observed loss of surface exposure was due to diminished secretory trafficking and not to defects in membrane insertion. These experiments indicate that manipulating the hydrophobicity and/or aromaticity of the TMD influences EMD-GFP's transit to the cell surface.

## Emerin contains a conserved ER retention signal

The autonomous trafficking of emerin's TMD challenged our initial hypothesis that emerin's localization relies on the LEM domain. Because EMD βLEM-GFP cannot traffic despite containing the TMD, we wondered whether a sequence within the βLEM construct inhibits trafficking. We noted that removing the LEM domain exposed a highly charged and conserved motif (QRRR) on the N-terminus of the construct (Figure S2D). Poly-arginine (RXR) motifs are known negative regulators of ER-to-Golgi transit[13]; we therefore tested whether this unprotected RXR could explain the ER-restricted localization of βLEM-GFP. Indeed, further truncating the βLEM construct by deleting the QRRR (βLEMβQRRR) freed the protein from the ER (**Figure 2F-H**).

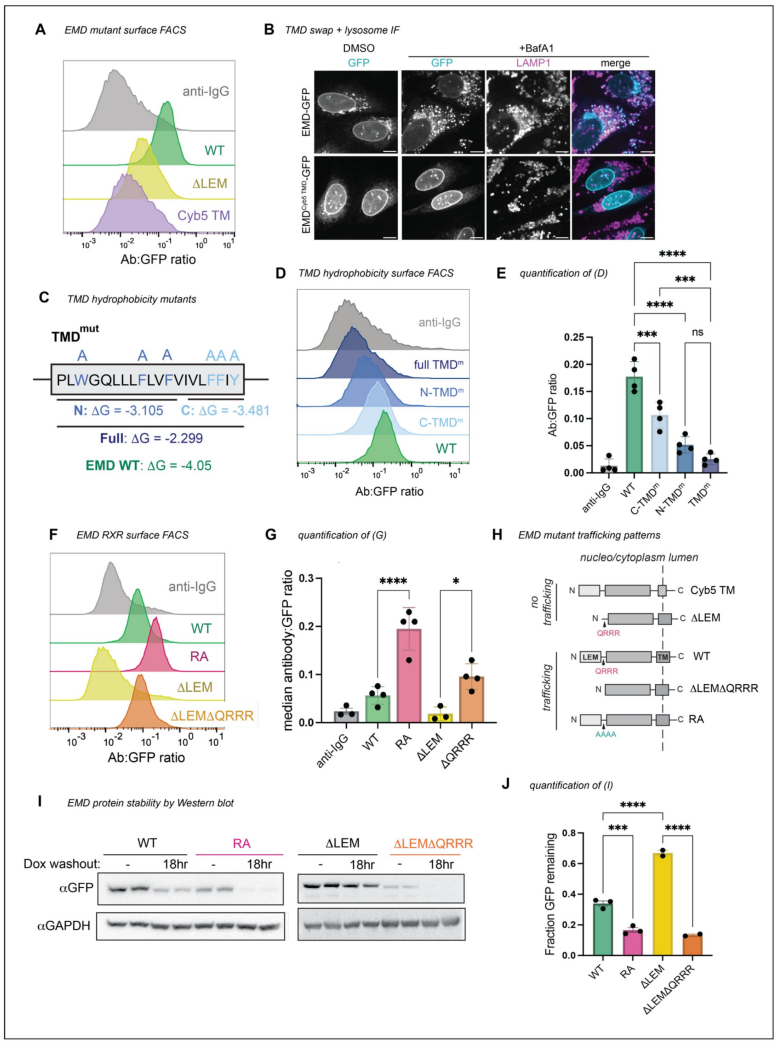


## Figure 2.

### Emerin's trafficking depends on its TMD, not on the LEM domain.

**A)** Surface anti-GFP antibody:GFP histogram of human WT EMD, βLEM, and EMD with mouse cytochrome B5 TMD (EMD$^{Cyb5\ TMD}$) chimera.

**B)** U2OS cells expressing mouse EMD-GFP and EMD$^{Cyb5\ TMD}$-GFP were induced with 1 ug/mL doxycycline for 24 hours, treated with 100nM lysosome blocking drug bafilomycin A1 (BafA1) overnight, and fixed and stained for lysosome marker Lamp1. Scale bars, 10 um.

**C)** TMD mutation strategy. The TM alpha helix of human EMD was divided into N-terminal and C-terminal halves, and the aromatic residues in each half were mutated to alanine to generate mutants with similar βG-insertion values. For the full TMD mutant, all aromatic residues were mutated to alanine, yielding a predicted βG-insertion of -2.299.

**D)** Surface antibody:GFP FACS histogram and **E)** quantification of the mutants diagramed in (C). *N* = 4 independent experiments

**F)** Surface antibody:GFP FACS histogram and **G)** quantification of mouse WT EMD, RA, βLEM, and βLEMβQRRR truncation surface expression. *N* = 4 independent experiments.

**H)** Summary of emerin constructs that do or do not traffic.

**I)** Western blot analysis of emerin constructs induced with 2 ug/mL doxycycline for 48 hours, then washed and incubated for an 18 hour chase.

**J)** Quantification of Western blot band intensity from (I). GFP antibody signal after washout was divided by the respective unwashed condition to yield the fraction GFP remaining after doxycycline washout across 3 independent replicates.

For all panels: *** indicates adjusted P-value <0.0005, * indicates P = 0.0104. All P-values were obtained by one-way ANOVA with Šídák's or Tukey's multiple comparisons tests.

To test whether the RXR motif limits the trafficking of full length EMD-GFP, we mutated the QRRR to AAAA (designated RA) and detected more flux to the PM compared to WT EMD-GFP (**Figure 2F-G**). Both βLEMβQRRR-GFP and EMD RA-GFP were less abundant at steady-state and were more rapidly degraded after removal of doxycycline from the medium (**Figure 2I-J**), suggesting increased flux to the lysosome. These data indicate that the RXR motif constitutes an ER retention sequence in EMD-GFP that is strengthened by the removal of the LEM domain. We infer that the presence of the LEM domain modulates the accessibility of the RRR motif; while the LEM domain itself is in fact dispensable for trafficking, its removal constitutively exposes the RRR motif, enhancing emerin's ER localization.

We next investigated the interplay between emerin's pro-trafficking TMD and its anti-trafficking RXR motif by cloning the RA mutation into our TMD mutant constructs (see **Figure 2C-E**). The RA mutation generally increased the surface expression of the TMD mutants except for the construct with the lowest hydrophobicity score ($TMD^{m}$), which was not significantly altered by the RA mutation (**Figure 3A-B**). We infer from this that the TMD acts upstream of the RXR motif in emerin's secretory trafficking, fitting with the hypothesis that low TMD hydrophobicity suffices to stably retain proteins in the ER[8].

Emerin is not the only tail-anchored INM protein with a particularly hydrophobic TMD. Another such protein is LAP2β[14], which shares several sequence features with emerin[15] (Figure S2A, 3C). We identified three RXR motifs within the LAP2β N-terminal domain, one of which (designated RXR1) is just downstream of the LEM-like fold—a striking similarity to emerin's RXR motif (**Figure 3C**). To test whether the same localization mechanisms govern LAP2β, we tagged its C-terminus with GFP and expressed it in U2OS cells. LAP2β-GFP was detected at the cell surface, albeit at much lower levels than EMD-GFP (**Figure 3D-E**, S3A-B). Interestingly, replacing most of the LAP2β N-terminal domain with the soybean ascorbate peroxidase (APEX2) enzyme caused a 20- fold increase in PM expression (**Figure 3D**, S3B), suggesting that the LAP2β TMD has a similar proclivity for secretory trafficking. Finally, mutating the LAP2β RXR1 to AAA led to a 70% increase in PM accumulation (**Figure 3D**), mirroring the effect of the EMD RA mutation. Together, these data indicate that the emerin and LAP2β TMDs are insufficient for NE/ER targeting and that both proteins contain retention sequences which counteract TMD-dependent secretion.

RXR motifs are thought to bind COPI subunits to return escaped proteins to the ER[13,16], though this mechanism is not understood. To test whether the increased trafficking of the RA mutant results from reduced COPI interaction, we immunoprecipitated N-terminally FLAG-tagged mouse emerin constructs from U2OS cells (Figure S3C). Mass spectrometry revealed a robust interaction between emerin and the COPI coat, with several COPI subunits ranking among the top hits (**Figure 3F**). Surprisingly however, this interaction was not weakened by the RXR mutation (**Figure 3G**). We noted that the mouse EMD bait also co-immunoprecipitated endogenous human EMD (**Figure 3G**), opening the possibility that COPI might indirectly interact with both FLAG constructs via endogenous emerin. Alternatively, the RXR motif's function could depend on protein topology. Importantly, while we were able to detect FLAG-EMD in the lysosome by IF (Figure S3D), FLAG- RA construct was not poorly expressed relative to FLAG-WT (Fig. S3C) in contrast to RA-GFP compared to WT-GFP (**Fig. 2I**). We also noted that the lysosomal accumulation of N-terminally FLAG-tagged emerin was more subtle than the C-terminally GFP-tagged version (**Figures 1A**, 2B), indicating that epitope tagging and/or tag orientation influences the extent of emerin protein turnover.

## C-terminal tagging destabilizes emerin via secretory trafficking

To determine whether tagging and/or overexpression increase the extent of emerin trafficking, we needed a system to better control emerin expression. To this end, we generated a human iPSC line with a dual integrase cassette exchange (DICE) landing pad[17] in the AAVS1 safe harbor locus (**Figure 4A**), then knocked emerin out of these cells with CRISPR/Cas9 (**Figure 4B**). Integrating GFP-tagged constructs into the parental and EMD KO DICE landing pads enabled us to measure

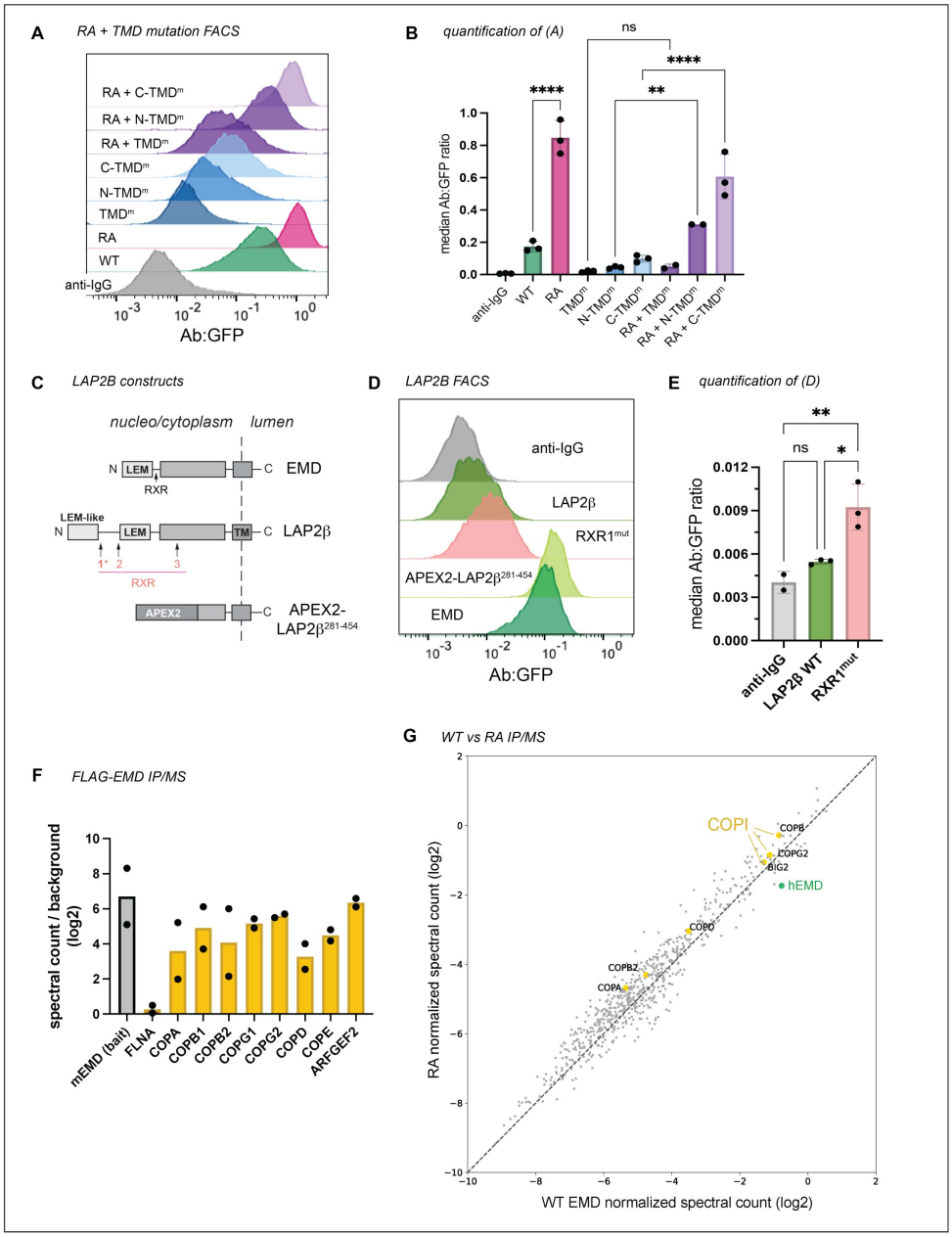


## Figure 3.

### RXR motif limits TMD-dependent trafficking of emerin and LAP2β without influencing COPI binding.

A) Surface anti-GFP:GFP histogram and **B)** quantification of indicated RA + TMD mutant combinations. ** indicates P = 0.0021. *N* = 3 independent experiments.

**C)** Diagram of LAP2β domain structure and position of RXR motifs. APEX2 fusion contains no RXR motifs.

**D)** Antibody:GFP histogram and **E)** quantification of the highest 25% GFP-expressing cells diagramed in (C). $RXR^{mut}$ : LAP2β RXR1 mutated to AAA. * indicates P = 0.0173; ** indicates P = 0.0072

**F)** Spectral counts of COPI proteins immunoprecipitated by WT FLAG-EMD normalized to negative control IP. Spectral counts of the mouse EMD bait and common contaminant filamin A (FLNA) plotted for comparison. *N* = 2 independent experiments.

**G)** Spectral counts of proteins immunoprecipitated by FLAG-WT and FLAG-RA mouse EMD normalized to each respective bait. Dotted line represents equal co-immunoprecipitation with the two constructs. COPI proteins and endogenous human EMD highlighted in yellow and green, respectively.

All P-values were obtained by one-way ANOVA with Šídák's or Tukey's multiple comparisons tests.

EMD-GFP trafficking in the presence or absence of the endogenous copy, respectively (**Figure 4C**). We included an mCherry-P2A upstream of the EMD-GFP to control for minor differences in construct expression (**Figure 4A**). The GFP-tagged emerin constructs mirrored the trafficking pattern we observed in U2OS cells; the EMD RA-GFP construct accumulated more at the PM, while the TMD mutant did not traffic (**Figure 4D-E**). The steady state abundance reflected these trafficking patterns. The GFP fluorescence of the TMD mutant accumulated to higher levels, indicating that it was stabilized by its inability to traffic. In contrast, the RA mutant fluorescence was slightly lower, indicating that it was modestly less stable than the WT protein, although this difference is not statistically significant (**Figure 4F-G**). There was no difference in total or surface expression between integrants in the EMD knockout and WT DICE backgrounds, suggesting that the trafficking of EMD-GFP is comparable both when moderately overexpressed and when expressed at endogenous levels (**Figure 4D-E**).

Tracking tail-anchored (i.e. untagged/N-terminally tagged) emerin through the secretory pathway is challenging because it lacks a lumenal domain amenable to surface labeling. However, after discovering ways to limit lysosomal flux (via the TMD) or accelerate it (via the RXR motif), we reasoned that the trafficking patterns of tail-anchored mutants could be inferred from their steady state abundance when expressed from the DICE landing pad. To test whether the GFP tag orientation affects protein expression, we compared the steady state fluorescence of N- and C-terminally tagged mutants. Surprisingly, the N-terminally tagged (tail-anchored) GFP fusions were 4-5 times more abundant than the C-terminally tagged (single pass) fusions (**Figure 4F-G**). C-terminal fusions were also more completely relocalized to the lysosome after BafA1 than N-terminal fusions, where NE/ER EMD signal was still apparent (Figure S4A). Unlike the C-terminal fusions, the N-terminally tagged TMD mutant did not accumulate more than the N-terminally tagged WT protein, suggesting that N-terminally tagged emerin is not destabilized by trafficking. We interpret this finding with caution, as we observed a slight decrease in the level of the N-terminally tagged TMD mutant compared to WT (**Figure 4G**). Since the insertion of tail-anchored proteins relies on TMD hydrophobicity[1,18], improper targeting to the ER membrane due to TMD mutation would confound our conclusion that N-terminally tagged constructs undergo similarly low levels of trafficking. Interestingly, upon treatment with BafA1, the N-terminally tagged WT and RA constructs formed GFP+ lysosomal puncta, while the N-terminally tagged TMD mutant did not (Figure S4A). This suggests that N-terminally tagged emerin does undergo some level of TMD- dependent trafficking. Further, the N-terminal RA fusion was slightly less fluorescent at steady state than WT (**Figure 4G**), indicating that the RXR motif also stabilizes tail-anchored GFP-EMD.

Because of the profound differences in the distribution of N and C-terminally tagged constructs, we investigated how lumenal GFP affects emerin's early secretory trafficking by analyzing its enrichment in ER exit sites (ERES). ER cargoes that are actively packaged into ERES can be distinguished from bulk flow secretory cargoes by incubating cells at 10C, where ERES form and cargoes accumulate but cannot progress toward the Golgi[19]. We compared the colocalization of endogenous untagged emerin, WT-GFP, and $TMD^{m}$-GFP with the ERES marker SEC31 at 37C and 10C (Figure S4B-C). We found that GFP-tagged emerin colocalized with SEC31 at steady- state, while this was not the case for endogenous emerin or the tagged TMD mutant. ERES colocalization was not increased at 10C for any of the emerin variants analyzed, indicating that emerin does not contain specific ER exit signals.

Collectively, these data indicate that N- and C-terminally tagged emerin constructs travel to the lysosome via their hydrophobic TMDs, although C-terminal tags accelerate this trafficking by encouraging bulk-flow ER exit.

Finally, we integrated untagged WT, RA, and TMD mutant constructs into EMD KO landing pad cells, then fixed and stained cells for confocal microscopy and flow cytometry. We saw no apparent differences in the localization or intensity of any of the emerin mutants, though the data

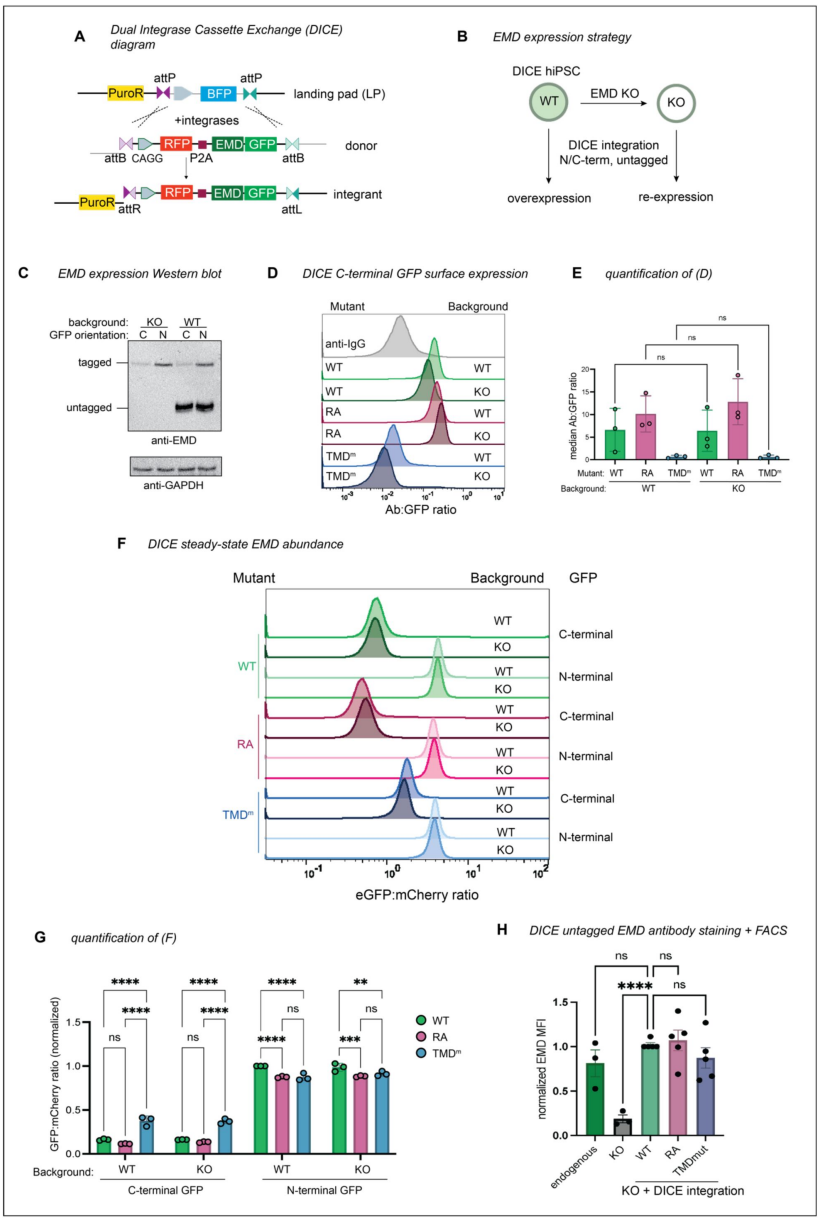


## Figure 4.

### Safe harbor expression reveals that C-terminal GFP destabilizes emerin.

**A)** Diagram of emerin integration into the AAVS1 locus. Landing pad BFP is exchanged for mCherry-P2A-emerin +/- GFP via Bxb1 and PhiC31 integrases. Integrases irreversibly recombine landing pad attP and donor attB sites into attR and attL sites.
**B)** Strategy to compare overexpressed emerin to knockout (KO) rescue.
**C)** Western blot analysis WT and EMD KO DICE hiPSCs expressing N- and C-terminally GFP-tagged emerin. Untagged endogenous EMD and GFP-tagged EMD are detected by the same anti-EMD antibody.
**D)** Anti-GFP surface labeling histogram and **E)** quantification of C-terminally tagged emerin integrants from (B-C). Statistical significance was determined using one-way ANOVA with Šídák's multiple comparisons test. *N* = 3 independent experiments.
**F)** FACS plot and **G)** quantification of steady state GFP abundance. Data were normalized to the GFP-EMD signal in the EMD WT background. *N* = 3 independent experiments. ** indicates P = 0.0079 by two-way ANOVA with Tukey's multiple comparisons test.
**H)** DICE landing pad WT, EMD KO, and KO re-integrated with untagged constructs were lifted, fixed, and stained with anti-EMD antibody. Fluorescence was quantified by flow cytometry and normalized to the WT DICE integrant. MFI, median fluorescence intensity of antibody signal. *N* = 5 replicates over 4 independent experiments. **** indicates P <0.0001 by mixed effects analysis.

were considerably noisier than the steady state GFP measurements (**Figure 4H**). We were also unable to detect untagged emerin in the lysosome after BafA1 treatment (Figure S4D), suggesting it does not traffic through the secretory pathway. However, the sensitivity of these assays may be limited by fixation, permeabilization, and antibody staining; therefore, we cannot rule out the possibility that small differences do exist between untagged emerin variants.

## Discussion

In this work, we dissected how exogenous epitope tags and intrinsic sequence elements influence the secretory trafficking of the INM resident protein emerin. We discovered that the aromatic amino acids in emerin's 23-residue TMD facilitate its travel to the lysosome. In the absence of other signals, TMD length and hydrophobicity are sufficient to partition tail-anchored proteins along the secretory pathway[8,9]. The biophysical properties of the emerin and LAP2β TMDs resemble PM, rather than ER, resident TMDs (Figure S2, ref.[11]). However, this notable hydrophobicity is likely important for the proteins' biogenesis. Tail-anchored proteins with very hydrophobic transmembrane domains are post-translationally targeted by the TRC40/GET complex, which captures C-terminal alpha helices after they emerge from the ribosome and delivers them to the ER membrane[1]. Emerin and Lap2β are established TRC40 client proteins[20,21], so their hydrophobic TMDs are likely required for TRC40 recognition. However, adding a C- terminal GFP converts a tail-anchored protein to a single-pass transmembrane protein, which will instead be co-translationally targeted to the ER by the SRP pathway[18,22]. Our results indicate that this change in topology displaces emerin, making C-terminally tagged emerin less stable and more prone to lysosomal trafficking than its N-terminally tagged counterpart (**Figure 4F-G**, S4A). Consistently, we found that only lumenally tagged emerin sampled ER exit sites, and that this was reduced by manipulating the TMD hydrophobicity (Figure S4B-C). This suggests that hydrophobic TMDs are less energetically favored within the ER membrane when attached to a lumenal domain, or that different biogenesis pathways bias cargoes toward ER exit.

We hypothesize that active ER retention plays a role in INM protein targeting. In interphase, emerin is not entirely sequestered at the INM by the nuclear lamina; a pool of emerin protein remains in the peripheral ER[23,24]. The intrinsic ability of emerin's TMD to traffic from the ER implies that a limiting mechanism must exist to bias the protein toward diffusion to the INM. Emerin could stably reside in the ER in part by binding to other ER-resident proteins. Interestingly, emerin was reported to interact with the ER tethering protein MOSPD3 via its YEESY (95-99) motif[25], which we previously found to limit trafficking[5]. While both TMDs traffic to the plasma membrane, full- length LAP2β-GFP is more retained in the NE/ER than EMD-GFP (**Figure 3D**, S3A-B), indicating that the N-terminal domains limit trafficking to different extents.

We identified the RXR motif as a shared negative regulator of TMD-dependent trafficking, prompting us to revise our original model: the exposure of this motif, not the absence of the LEM domain, prevents ER exit of EMD-GFP (**Figure 2F-G**). This suggests that the sequences around the RXR motif influence its activity by steric occlusion or other mechanisms. RXR motifs prevent the ER exit of some PM-resident proteins until they are masked by oligomerization, thus coupling ER exit to folding and/or assembly[13]. Like the canonical ER retrieval motif KKXX, RXR motifs are thought to engage COPI subunits to return escaped ER membrane proteins from the early Golgi[13,26]. Yeast-2-hybrid experiments predicted RXR signals to interact with the beta and delta subunits of the COPI coat[16], though the molecular details are still unclear. Contrary to KKXX motifs, found only on C-termini, RXR motifs may be on N-termini or within a poly-peptide chain[13]. Truncated, lumenally tagged variants of Sun2, another tail-anchored INM protein, require a poly- arginine motif to prevent mislocalization to the Golgi[27]. Turgay et al[27]. observed purified Sun2 RXR mutants losing interaction with COPI subunits in GST pull-down assays. In contrast, we did not observe loss of COPI binding in our RXR mutant immunoprecipitations. This discrepancy may be explained by differences in methods (purified

recombinant protein binding assays vs. native IP), or by oligomerization of tagged emerin with endogenous emerin to indirectly bind COPI in lysate[28]. Emerin's interaction with the COPI coat was recently detected by proximity biotinylation in mouse P19 cells[29]. Interestingly, emerin was the only non-Golgi resident protein identified in the gamma- COP subunit interactome, indicating that endogenous emerin might be a COPI cargo. While we predict this interaction occurs via emerin's RXR motif, we cannot exclude the possibility of other COPI-interacting mechanisms.

Our previous work identified EMD as an unstable protein subject to significant lysosomal flux[5]. However, we have now discovered that emerin's trafficking is markedly promoted by C-terminal GFP tagging, likely influencing many of our initial observations. While we used C-terminal tags to avoid disrupting emerin's N-terminal interactions with chromatin and lamins, this approach inadvertently altered its localization. We did detect trafficking of N-terminally tagged emerin, but found that it occurs at a much lower rate. We conclude that hydrophobic tail-anchored transmembrane domains are readily dislocated by C-terminal tags, and echo the warnings raised by generations of cell biologists regarding tag-induced localization artifacts[30–32]. We did not detect trafficking of the untagged emerin constructs. Nonetheless, because trafficking is detectable at or below endogenous levels with different tags and orientations, we cannot rule out the possibility that emerin traffics under specific conditions. We note poor correlation of emerin transcript and protein across tissues[33] (Figure S4E), which suggests protein-level regulation that may dynamically regulate emerin levels. While we still do not know whether emerin's ability to travel beyond the NE/ER influences its function, our experiments reveal an unanticipated connection between the topology and localization of INM proteins and raise new questions about the balance between secretion and retention of INM-destined proteins.

# Methods

## Cell culture and cell line generation

U2OS cells were obtained from the UCSF Cell and Genome Engineering Core and were cultured in McCoy's 5A medium supplemented with 10% FBS and penicillin/streptomycin. To generate EMD-GFP cell lines, U2OS were seeded into 6-well plates at a density of 300,000 cells per well. The next day, a transfection mix of 0.5 ug EMD-GFP donor plasmid, 0.25 ug PB200A-1 PiggyBac Transposase plasmid, 3.5 uL Lipofectamine 2000, and 300 uL Optimem was added to each well. After 24 hours, cells were split 1:2 and selected in 5 ug/mL blasticidin for 1 week, then maintained in 5 ug/mL blasticidin thereafter. Prior to an experiment, cells were split into media without blasticidin and induced with 1 ug/mL doxycycline for 24-48 hours. To generate FLAG-EMD cell lines, 2 ug CMV-FLAG-EMD plasmid was transfected without PiggyBac Transposase. Cells were selected with 400 ug/mL G418 for one week, then maintained in 200 ug/mL G418.

WTC-11 hiPSCs were obtained from the Berkeley Stem Cell Center. Cells were maintained on Matrigel-coated vessels in mTeSR+ without penicillin/streptomycin. Cells were passaged as clumps (using ReLeSR) for routine culture and as single cells (using Accutase) for counting and electroporating. Cells were plated in ROCK inhibitor Y-27632, then changed to fresh mTeSR+ after 24 hours. CRISPR editing was performed by electroporating 12.5 pmol pure Cas9-NLS and 12.5 pmol sgRNA into 1 million cells using a 100 uL Neon electroporator set to 1300 V, 30 ms, and 1 pulse. For DICE landing pad installation, we included 2 ug cassette-containing HDR template plasmid in the transfection mix. Landing pad cells were selected in 0.25 ug/mL puromycin for 3 days. Single clones were isolated by limiting dilution in 96 well plates, then expanded and genotyped for heterozygous insertion using primers spanning the AAVS1 homology arms. Emerin knockouts were generated from one landing pad clone using two sgRNAs targeting the start and end of the coding sequence. Clones were genotyped by PCR to verify the entire region was deleted, then by Western blot to confirm the loss of protein. To integrate emerin constructs into the DICE landing pad, we electroporated 1 million cells with 2 ug attB-containing donor plasmid and 500 ng

BxbI-P2A-PhiC31 integrase plasmid. After letting cells recover, we isolated landing pad BFP–/donor+ cells using a SONY SH800 cell sorter. Cells were checked for mycoplasma every 3-4 months and were found to be negative.

## Plasmid cloning

All U2OS constructs except FLAG-EMD were expressed in the XLone all-in-one Tet-ON Piggybac plasmid[34]. Mouse emerin sequences were cloned into XLone from plasmids used in our previous study. Human emerin and LAP2β were amplified from Hek293T and WTC-11 cDNA using primers with overhangs to XLone. Mouse cytochrome B5 was amplified from E14 mESC cDNA. cDNA was synthesized using NEB MMLV reverse transcriptase. FLAG-EMD constructs were expressed from the CMV promoter in a Neo/Kan resistant vector.

## Emerin constructs

| Designation | Gene | Species | Uniprot ID | Mutation |
|---|---|---|---|---|
| LAP2β RXR1 | LAP2β | Human | P42167 | 48-50 -> AAA |
| LAP2β APEX2-TMD | LAP2β | Human | P42167 | 1-280 -> APEX2 |
| hEMD RA | EMD | Human | P50402 | 44-47 -> AAAA |
| hEMD ΔLEM | | Human<br>Mouse | P50402<br>O08579 | D1-43 |
| hEMD ΔLEM<br>ΔQRRR | EMD | Human<br>Mouse | P50402<br>O08579 | D1-47 |
| hEMD Cyb5 TM | EMD | Human | P50402 (EMD)<br>P56395 (Cyb5) | EMD 1-224 + mouse cyb5a 95-134 |
| mEMD Cyb5 TM | EMD | Mouse | O08579 (EMD)<br>P56395 (Cyb5) | EMD 1-225 + mouse Cyb5a 95-134 |
| TMD-GFP | EMD | Mouse | O08579 | 212-259 |
| N-TMD$^{m}$ | EMD | Human | P50402 | W226A ,F232A, F235A |
| C-TMD$^{m}$ | EMD | Human | P50402 | F240A, F241A, Y243A |
| Full TMD$^{m}$ | EMD | Human | P50402 | W226A ,F232A, F235A, F240A, F241A, Y243A |

Small emerin mutations were generated using the NEB site-directed mutagenesis kit, while larger fusions were assembled using the NEB HiFi Assembly kit.

The DICE landing pad cassette contained a PGK promoter driving HSV thymidine kinase-P2A-TagBFP, all flanked by BxbI and PhiC31 attP sites. This cassette was built into an AAVS1 targeting vector (a generous gift from Dr. Tom Nowakowski) containing a splice acceptor-P2A-puro. DICE donor constructs contained Bxb1 and PhiC31 attB sites flanking the CAGGS promoter and an mCherry-P2A-EMD.

Plasmids were prepped using the ZymoPURE II midiprep kit. All plasmids were verified by Sanger or whole plasmid nanopore sequencing before transfection.

## Transmembrane domain hydrophobicity calculations

Transmembrane segments were obtained for EMD, LAP2β, STX3, and CYB5 from Uniprot annotations. DG-ins was calculated using the DGprediction algorithm[35]. Median DG-transfer and TM length values for secretory membranes were obtained from the human Membranome database[14,36]. Data obtained from the Membranome database were plotted in GraphPad Prism.

## Surface labeling and flow cytometry

The surface staining assay was adapted from Welch et al[37]. Briefly, cells were washed with PBS, lifted for 3-5 minutes with accutase, then quenched with cold complete media. Cells were transferred to microfuge tubes and placed on ice for the duration of staining and washing. Cells were pelleted 800g for 3 minutes at 4C, then washed once in 2% FBS/PBS. Cells were stained in 80 uL anti-GFP 647 (1:20 in 2% FBS/PBS) or anti-rabbit IgG Alexa Fluor 647 secondary antibody (1:200 in 2% FBS/PBS) as a negative control. The cells used for the anti-IgG controls were WT EMD-GFP (for all EMD comparisons) or WT LAP2β-GFP (for LAP2β comparisons). After staining for 30 minutes, cells were diluted with 200 uL 2% FBS/PBS, pelleted and washed twice with 400 uL 2% FBS/PBS, and then optionally fixed in 4% PFA/PBS for 10 minutes at room temperature. Fixed cells were washed twice and then stored at 4C until being resuspended in PBS and strained into round bottom FACS tubes before analysis.

For flow analysis of antibody-stained proteins, cells were lifted with accutase, washed with PBS, and fixed by rotating in 4% PFA/PBS for 10 minutes. After washing twice in PBS, cells were permeabilized in IF buffer (0.1% Tx100, 0.02% SDS, 10 mg/ml BSA in PBS) for 30 minutes before incubating in primary antibody solution for 1-2 hours at room temperature. Cells were washed three times in IF buffer, incubated with fluorescent secondary antibodies for 1 hour, and then washed three more times before being strained into FACS tubes.

Cells were analyzed on a BD FACSVerse or a ThermoFisher Attune NxT. At least 50,000 cells were analyzed per sample. Flow cytometry data were analyzed in FlowJo. Surface antibody:GFP ratio was obtained using the “derive parameters” function and applied to the GFP+ populations. Histograms are normalized to the mode of each sample for visualization.

## Immunofluorescence microscopy

Cells were seeded in Ibidi culture chambers (Matrigel-coated for hiPSCs) prior to an IF experiment. For lysosome colocalization analysis, cells were treated with 100 nM bafilomycin A1 for 16-18 hours. Cells were washed in PBS, then fixed in 4% paraformaldehyde in PBS for 5 minutes at room temperature. For LAMP1 staining, cells were permeabilized in 0.1% digitonin/PBS at 4 C for 10 minutes, then blocked in 2% FBS/PBS. LAMP1 antibody was diluted 1:200 in 2% FBS/PBS. For emerin and FLAG immunostaining, fixed cells were permeabilized in IF buffer for 30 minutes, then incubated in primary antibodies (diluted 1:250 and 1:1000 in IF buffer, respectively) for 1 hour at room temperature. After washing, cells were incubated with Alexa-Fluor-conjugated secondary antibodies and Hoechst 33342 (both 1:1000) for 30 minutes at room temperature. Emerin/FLAG staining is incompatible with LAMP1 staining because of differential permeabilization requirements. In these cases, we had to rely on the formation of EMD+ puncta after bafilomycin treatment to infer lysosome localization.

Selective permeabilization and ERES co-localization temperature blocks were performed as previously described[38]. For selective permeabilization topology analysis, U2OS cells were induced with doxycycline for 24 hours, washed with cold PBS, and incubated with cold 0.0025% digitonin/PBS or PBS only for 5 minutes at 4C. Cells were then fixed with 4% PFA for 5 minutes at

RT. To permeabilize all endomembranes, cells were incubated with IF buffer (0.1% Tx100, 0.02% SDS, 10 mg/ml BSA in PBS for 30 minutes, then stained with anti-EMD and anti-GFP antibodies diluted in 2% FBS/PBS.

For ERES co-localization, EMD-GFP U2OS cells were were induced with doxycycline for 4 hours or left uninduced to analyze newly synthesized or endogenous emerin, respectively. Cells were then placed on a metal platform submerged in a 10C water bath or continued incubation at 37C for 2 hours, then fixed and stained for endogenous emerin and Sec31a to mark ERES.

Images were acquired using a Nikon CSU-X1 spinning disk confocal microscope with 40x/1.3 NA or 60x/1.4 NA oil objectives. 20-30 Z-slices were imaged per cell with a step size of 0.3 microns. 16-bit images were saved as ND2 files using the Nikon Elements 5.02 build 1266 software. Representative slices were selected and cropped in FIJI. Pearson correlation was calculated using the FIJI PSC colocalization plugin.

## Protein stability measurement and Western blotting

For doxycycline washout experiments, 300,000 U2OS cells were seeded in 12 well plates with 2 ug/mL doxycycline. After 48 hours, half the wells were washed twice with PBS and incubated in fresh medium without doxycycline for 18 hours. Cells were washed twice with PBS and lysed in the wells by scraping in 80 uL RIPA buffer (50mM Tris, 150mM NaCl, 1% TritonX-100, 0.5% deoxycholate, 0.1% SDS) plus protease inhibitors and benzonase. Lysates were spun 17,000g at 4C for 10 minutes, then supernatants were mixed with sample buffer and boiled for 10 minutes. 12 uL of each sample was loaded onto homemade 10% SDS-PAGE gels, then transferred onto nitrocellulose membranes. Blots were incubated at 4C overnight in primary antibody diluted with 5% milk/TBST, then washed and incubated in HRP-conjugated secondary antibodies for 1 hour at room temperature. Blots were developed using Pierce ECL Western blotting substrate and imaged using the GelDoc imaging system. Band intensity was quantified in Fiji.

## FLAG-EMD immunoprecipitation and mass spectrometry

FLAG-EMD, FLAG-RA, and parental U2OS (non-expressing negative control) cells were grown to confluence in 3 10cm plates per cell line, then harvested by scraping and transferring to a microfuge tube. Cells were pelleted and lysed in 1 mL lysis buffer (50 mM Tris-HCl pH 7.4, 150 mM NaCl, 0.3% TritonX-100, 1 mM DTT, 2 mM EDTA, 5 mM MgCl2, 1x protease inhibitor cocktail, 1x PhosSTOP, benzonase), then incubated for 30 minutes end over end at 4C. Lysates were probe sonicated in 6 rounds of 10 second pulses at 20% power, then spun 17,000g at 4C for 25 minutes. The supernatant was added to 40 uL FLAG M2 magnetic beads which had been calibrated in 500 uL lysis buffer and separated on a magnetic stand. Samples were incubated end over end at room temperature for 1 hour, then magnetically separated and washed 3 times with 1 mL wash buffer (100 mM HEPES-KOH pH 7.5, 100 mM KCl, 5% glycerol, 0.1% NP-40, protease inhibitors). After the final wash, the supernatant was discarded and the beads were resuspended in 200 uL elution buffer (100 ug/mL 3x FLAG peptide in wash buffer) and eluted for 1 hour at room temperature. Eluates were precipitated with 4 volumes ice cold acetone overnight at -20C, spun at max speed for 5 minutes, then air dried. Pellets were processed for mass spectrometry using a PreOmics iST kit according to manufacturer's instructions.

## Mass spectrometry and analysis

A nanoElute was attached in line to a timsTOF Pro equipped with a CaptiveSpray Source (Bruker, Hamburg, Germany). Chromatography was conducted at 40°C through a 25 cm reversed-phase C18 column (PepSep) at a constant flowrate of 0.5 µL $min^{-1}$. Mobile phase A was 98/2/0.1% water/MeCN/formic acid (v/v/v) and phase B was MeCN with 0.1% formic acid (v/v). During a 108

min method, peptides were separated by a 3-step linear gradient (5% to 30% B over 90 min, 30% to 35% B over 10 min, 35% to 95% B over 4 min) followed by a 4 min isocratic flush at 95% for 4 min before washing and a return to low organic conditions.

Experiments were run as data-dependent acquisitions with ion mobility activated in PASEF mode. MS and MS/MS spectra were collected with $m/z$ 100 to 1700 and ions with $z$ = +1 were excluded. Raw data files are available on the Mass Spectrometry Interactive Virtual Environment (MassIVE), a full member of the Proteome Xchange consortium under the identifier: MSV000096858.

Raw data files were searched using PEAKS Online Xpro 1.6 (Bioinformatics Solutions Inc., Waterloo, Ontario, Canada). The precursor mass error tolerance and fragment mass error tolerance were set to 20 ppm and 0.03 respectively. The trypsin digest mode was set to semi-specific and missed cleavages was set to 2. The human Swiss-Prot reviewed (canonical) database (downloaded from UniProt) totaling 20,385 entries or a custom database using human and mouse emerin (downloaded from uniprot, EMD_human P50402, EMD_mouse O08579) was used. Carbamidomethylation (C) was selected as a fixed modification. Oxidation (M) was selected as a variable modification.

Resulting datasets were subjected to the following filtration criteria: (1) Database search (−10 log($p$-value) ≥ 20, 1% peptide and protein FDR). (2) Identified proteins with less than 3% coverage, 3 unique peptides, or spectral areas less than 5000 were discarded. (4) Spectral counts for each protein were normalized to corresponding counts from the negative control IP, and then to the protein length. (5) The ratio of normalized counts to the mouse emerin bait was plotted to obtain relative co-immunoprecipitation efficiency.

## Acknowledgements

We are grateful to UCSF core facility staff for training and technical support. The Gladstone Institutes Stem Cell Core provided hiPSC culture training and equipment. Images were acquired at the Center for Advanced Light Microscopy- CVRI Microscopy core on microscopes purchased though the UCSF Research Evaluation and Allocation Committee, the Gross Fund, and the Heart Anonymous Fund. Flow cytometers and cell sorters were purchased and supported by the UCSF Center for Live Cell Analysis core.

We also thank Elphege Nora for guidance with integrase cassette exchange, Emmy Delaney for experimental assistance, and Tracy Knight for experimental assistance and feedback on this manuscript. Adam Frost, Shaeri Mukherjee, Peter Walter, Martin Kampmann, Willow Coyote-Maestas, and members of the Buchwalter lab provided valuable perspective and discussion throughout this work. A.B. was supported by the Chan Zuckerberg Biohub, and J.M. was supported by the National Heart, Lung, and Blood Institute (F31HL170757).

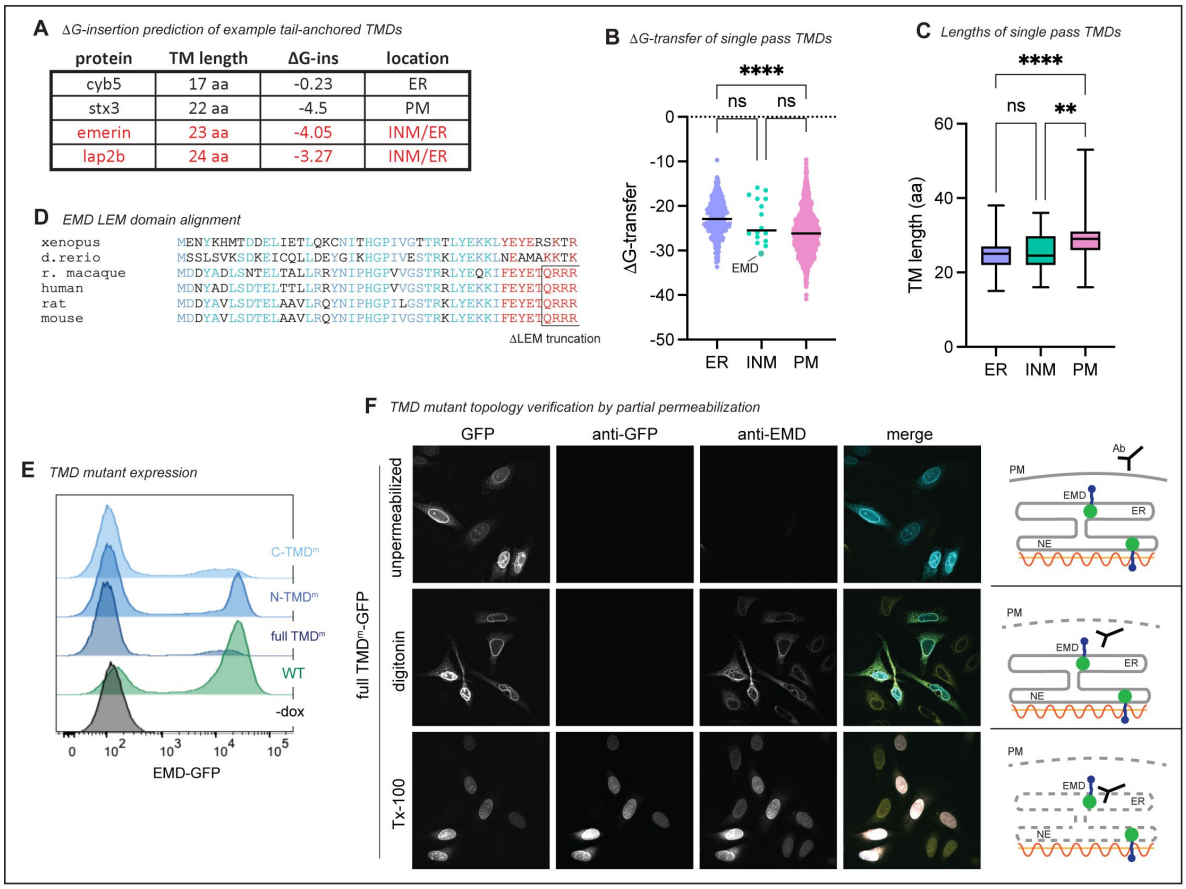


## Figure 2 supplement

**A)** Lengths and predicted βG-insertion values of ER protein cytochrome B5, PM protein syntaxin 3, and emerin INM proteins emerin and Lap2β.

**B)** Single pass human transmembrane proteins from Membranome database plotted by free energy of transfer into a lipid bilayer. Lines represent median; **** indicates P < 0.0001 by one-way Anova with Tukey's multiple comparisons test.

**C)** Transmembrane domain length (by amino acid count) of the proteins in (B). ** indicates P = 0.0028; **** indicates P < 0.0001.

**D)** Protein sequence alignment of emerin's LEM domain across species. Conserved LEM domain amino acid class indicated in blue. QRRR motif is conserved in mammals and is exposed in the βLEM construct.

**E)** FACS plots of WT EMD-GFP and TMD mutant expression upon dox induction. Fewer cells express C-TMD$^{m}$ and full TMD$^{m}$, though topology of constructs that are expressed is not altered (see (F).

**F)** Antibody accessibility upon differential permeabilization of U2OS cells expressing full TMD$^{m}$. Cells were incubated with digitonin to permeabilize the plasma membrane, TritonX-100 to permeabilize all internal membranes, or left unpermeabilized, then stained with antibodies against emerin (cytosolic epitope) and GFP (lumenal epitope).

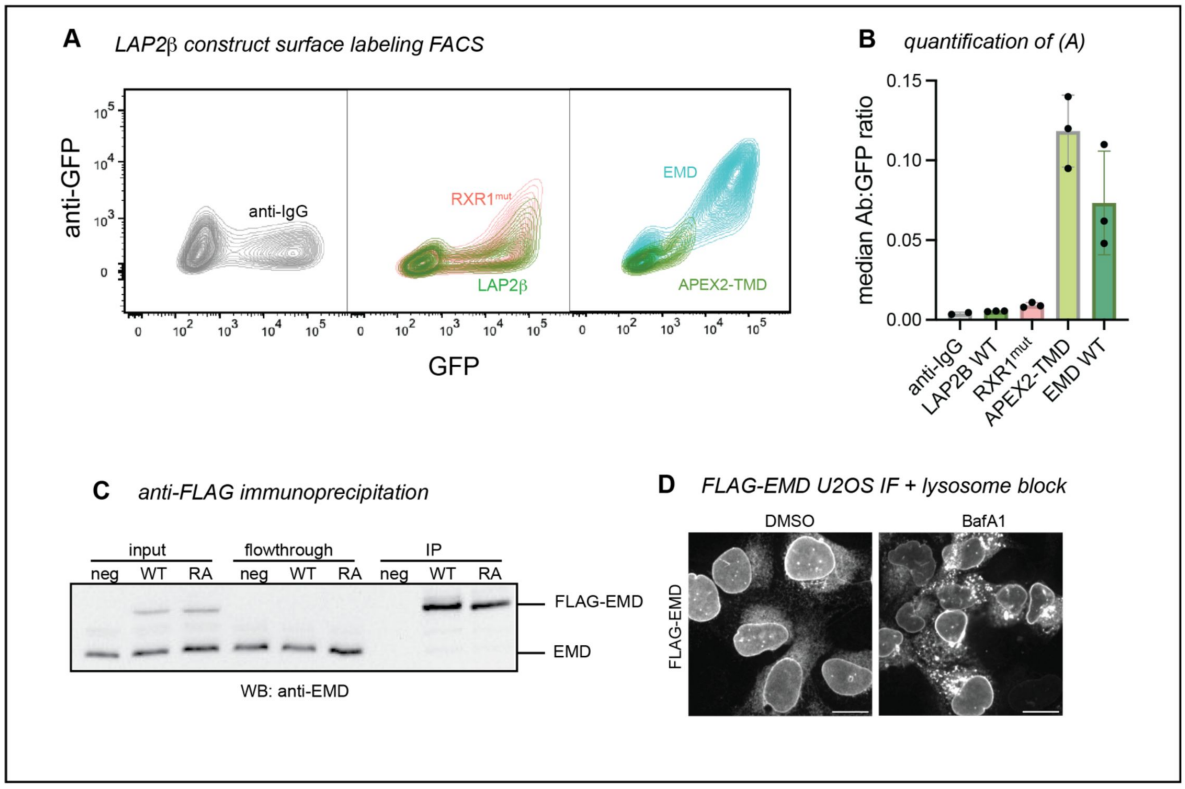


## Figure 3 supplement

**A)** GFP versus surface anti-GFP FACS plots of negative control anti-IgG, WT LAP2β / RXR1mut, and WT EMD / LAP2β APEX2-TMD.
**B)** Median anti-GFP antibody:GFP ratio of the highest 25% GFP-expressing cells in (A).
**C)** Western blot analysis of anti-FLAG immunoprecipitations. U2OS cells expressing no FLAG construct (neg), FLAG-WT mouse EMD, and FLAG-RA mutant were lysed and incubated with anti-FLAG magnetic beads. Equal volume equivalents were separated by SDS-PAGE and blotted with an anti-EMD antibody to visualize tagged and untagged EMD.
**D)** U2OS cells expressing FLAG-EMD were incubated with lysosome blocker bafilomycin A1 (BafA1) overnight, then fixed and permeabilized with 0.1% Triton-X-100, 0.02% SDS, 10 mg/ml BSA in PBS. Cells were stained with anti-FLAG antibody to visualize relocalization during BafA1 treatment. Scale bars, 20 um.

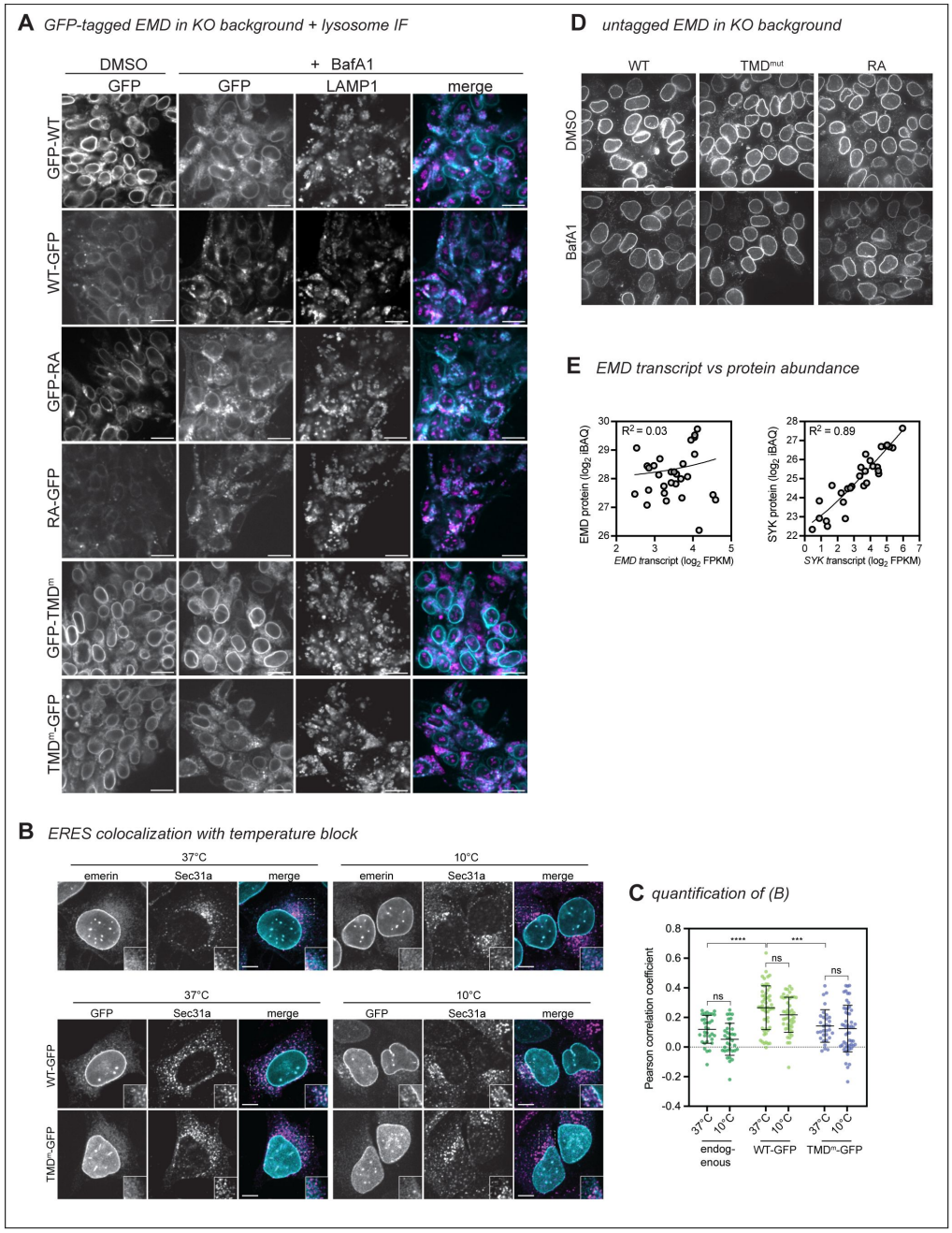


## Figure 4 supplement

**A)** EMD KO DICE hiPSCs were integrated with GFP-tagged EMD constructs. Cells were treated with vehicle or lysosome blocker bafilomycin A1 (BafA1) overnight, then fixed and stained with anti-LAMP1 antibody.
**B)** U2OS cells expressing indicated constructs were induced with doxycycline for 4 hours (bottom panels) or left uninduced (top panels). Cells were then shifted to 10C or continued incubation at 37C for 2 hours. Cells were then fixed and stained for endogenous emerin (top panel) and Sec31a to mark ERES.
**C)** Pearson correlation coefficient was calculated between endogenous emerin or EMD-GFP and Sec31a. *N* = 31-54 cells over 3 independent experiments. *** indicates P = 0.0006 by one-way ANOVA with Tukey's multiple comparisons test.
**D)** EMD KO DICE hiPSCs were integrated with untagged EMD WT, TMD mutant, or RA mutant. Cells were treated overnight with BafA1, then fixed and stained with anti-EMD antibody. Scale bars, 20 um.
**E)** We mined a dataset of matched RNAseq and quantitative protein abundances across 29 human tissues to evaluate EMD transcript and protein abundances. EMD protein and transcript abundance are largely uncorrelated (R2 ~ 0), while, for comparison, the enzyme spleen tyrosine kinase (SYK) has well-correlated protein and RNA levels (R2 = 0.89)

# References


1. Rapaport D., Herrmann J. M (2023) **Chasing the right tail: How the ER membrane complex recognizes its substrates** *Journal of Cell Biology* **222**:e202306035 Google Scholar

2. Boni A., et al. (2015) **Live imaging and modeling of inner nuclear membrane targeting reveals its molecular requirements in mammalian cells** *Journal of Cell Biology* **209**:705–720 Google Scholar

3. Ungricht R., Klann M., Horvath P., Kutay U (2015) **Diffusion and retention are major determinants of protein targeting to the inner nuclear membrane** *J Cell Biol* **209**:687–704 Google Scholar

4. Ellenberg J., et al. (1997) **Nuclear Membrane Dynamics and Reassembly in Living Cells: Targeting of an Inner Nuclear Membrane Protein in Interphase and Mitosis** *J Cell Biol* **138**:1193–1206 Google Scholar

5. Buchwalter A., Schulte R., Tsai H., Capitanio J., Hetzer M (2019) **Selective clearance of the inner nuclear membrane protein emerin by vesicular transport during ER stress** *eLife* **8**:e49796 https://doi.org/10.7554/eLife.49796 | Google Scholar

6. Satpute-Krishnan P., et al. (2014) **ER Stress-Induced Clearance of Misfolded GPI-Anchored Proteins via the Secretory Pathway** *Cell* **158**:522–533 Google Scholar

7. Lee K. K., et al. (2001) **Distinct functional domains in emerin bind lamin A and DNA-bridging protein BAF** *Journal of Cell Science* **114**:4567–4573 Google Scholar

8. Ronchi P., Colombo S., Francolini M., Borgese N (2008) **Transmembrane domain–dependent partitioning of membrane proteins within the endoplasmic reticulum** *J Cell Biol* **181**:105–118 Google Scholar

9. Borgese N (2016) **Getting membrane proteins on and off the shuttle bus between the endoplasmic reticulum and the Golgi complex** *Journal of Cell Science* **129**:1537–1545 Google Scholar

10. Bulbarelli A., Sprocati T., Barberi M., Pedrazzini E., Borgese N (2002) **Trafficking of tail-anchored proteins: transport from the endoplasmic reticulum to the plasma membrane and sorting between surface domains in polarised epithelial cells** *Journal of Cell Science* **115**:1689–1702 Google Scholar

11. Sharpe H. J., Stevens T. J., Munro S (2010) **A Comprehensive Comparison of Transmembrane Domains Reveals Organelle-Specific Properties** *Cell* **142**:158–169 Google Scholar

12. Pedrazzini E., et al. (2000) **Mechanism of residence of cytochrome b(5), a tail- anchored protein, in the endoplasmic reticulum** *J Cell Biol* **148**:899–914 Google Scholar

13. Michelsen K., Yuan H., Schwappach B. (2005) **Hide and run** *EMBO Rep* **6**:717–722 Google Scholar

14. Lomize A. L., Lomize M. A., Krolicki S. R., Pogozheva I. D (2017) **Membranome: a database for proteome-wide analysis of single-pass membrane proteins** *Nucleic Acids Res* **45**:D250–D255 Google Scholar

15. Berk J. M., Tifft K. E., Wilson K. L (2013) **The nuclear envelope LEM-domain protein emerin** *Nucleus* **4**:298–314 Google Scholar

16. Michelsen K., et al. (2007) **Novel cargo-binding site in the β and δ subunits of coatomer** *Journal of Cell Biology* **179**:209–217 Google Scholar

17. Zhu F., et al. (2014) **DICE, an efficient system for iterative genomic editing in human pluripotent stem cells** *Nucleic Acids Research* **42**:e34 Google Scholar

18. Shao S., Hegde R. S (2011) **Membrane Protein Insertion at the Endoplasmic Reticulum** *Annu Rev Cell Dev Biol* **27**:25–56 Google Scholar

19. Mezzacasa A., Helenius A (2002) **The Transitional ER Defines a Boundary for Quality Control in the Secretion of tsO45 VSV Glycoprotein** *Traffic* **3**:833–849 Google Scholar

20. Coy-Vergara J., Rivera-Monroy J., Urlaub H., Lenz C., Schwappach B (2019) **A trap mutant reveals the physiological client spectrum of TRC40** *J Cell Sci* **132**:jcs230094 Google Scholar

21. Pfaff J., et al. (2016) **Emery–Dreifuss muscular dystrophy mutations impair TRC40-mediated targeting of emerin to the inner nuclear membrane** *J Cell Sci* **129**:502–516 Google Scholar

22. Translocation of proteins across the endoplasmic reticulum (1981) **I. Signal recognition protein (SRP) binds to in-vitro-assembled polysomes synthesizing secretory protein** *J Cell Biol* **91**:545–550 Google Scholar

23. Nastały P., et al. (2020) **Role of the nuclear membrane protein Emerin in front-rear polarity of the nucleus** *Nature Communications* **11**:2122 Google Scholar

24. Salpingidou G., Smertenko A., Hausmanowa-Petrucewicz I., Hussey P. J., Hutchison C. J (2007) **A novel role for the nuclear membrane protein emerin in association of the centrosome to the outer nuclear membrane** *J Cell Biol* **178**:897–904 Google Scholar

25. Cabukusta B., et al. (2020) **Human VAPome Analysis Reveals MOSPD1 and MOSPD3 as Membrane Contact Site Proteins Interacting with FFAT-Related FFNT Motifs** *Cell Reports* **33** Google Scholar

26. Marcello E., Gardoni F., Luca M. D., Pérez-Otaño I (2010) **An Arginine Stretch Limits ADAM10 Exit from the Endoplasmic Reticulum *** *Journal of Biological Chemistry* **285**:10376–10384 Google Scholar

27. Turgay Y., et al. (2010) **A classical NLS and the SUN domain contribute to the targeting of SUN2 to the inner nuclear membrane** *The EMBO Journal* **29**:2262–2275 Google Scholar

28. Fernandez A., Bautista M., Pinaud F. (2021) **Emerin oligomerization and nucleoskeletal coupling at the nuclear envelope regulate nuclear mechanics against stress** *bioRxiv* https://doi.org/10.1101/2021.02.12.429834 | Google Scholar

29. Zhao X., et al. (2021) **ultraID: a compact and efficient enzyme for proximity-dependent biotinylation in living cells** *bioRxiv* https://doi.org/10.1101/2021.06.16.448656 | Google Scholar

30. Stadler C., et al. (2013) **Immunofluorescence and fluorescent-protein tagging show high correlation for protein localization in mammalian cells** *Nat Methods* **10**:315–323 Google Scholar

31. Montecinos-Franjola F., Bauer B. L., Mears J. A., Ramachandran R (2020) **GFP fluorescence tagging alters dynamin-related protein 1 oligomerization dynamics and creates disassembly-refractory puncta to mediate mitochondrial fission** *Sci Rep* **10** Google Scholar

32. Margolin W (2012) **The Price of Tags in Protein Localization Studies** *J Bacteriol* **194**:6369–6371 Google Scholar

33. Wang D., et al. (2019) **A deep proteome and transcriptome abundance atlas of 29 healthy human tissues** *Mol Syst Biol* **15**:e8503 Google Scholar

34. Randolph L. N., Bao X., Zhou C., Lian X. (2017) **An all-in-one, Tet-On 3G inducible PiggyBac system for human pluripotent stem cells and derivatives** *Sci Rep* **7**:1549 Google Scholar

35. Hessa T., et al. (2007) **Molecular code for transmembrane-helix recognition by the Sec61 translocon** *Nature* **450**:1026–1030 Google Scholar

36. Lomize A. L., Hage J. M., Pogozheva I. D (2018) **Membranome 2.0: database for proteome-wide profiling of bitopic proteins and their dimers** *Bioinformatics* **34**:1061–1062 Google Scholar

37. Welch L. G., Peak-Chew S.-Y., Begum F., Stevens T. J., Munro S (2021) **GOLPH3 and GOLPH3L are broad-spectrum COPI adaptors for sorting into intra-Golgi transport vesicles** *Journal of Cell Biology* **220** Google Scholar

38. Heyden Vander, Naismith A. B., Snapp T. V., Hanson E. L. (2011) **Static retention of the lumenal monotopic membrane protein torsinA in the endoplasmic reticulum** *The EMBO Journal* **30**:3217–3231 Google Scholar

## Author information

**Jessica Mella**
Cardiovascular Research Institute, University of California, San Francisco, San Francisco, United States
ORCID iD: 0000-0001-7541-6789

**Regan Volk**
Cardiovascular Research Institute, University of California, San Francisco, San Francisco, United States
ORCID iD: 0000-0001-6748-719X

**Balyn Zaro**
Cardiovascular Research Institute, University of California, San Francisco, San Francisco, United States, Department of Pharmaceutical Chemistry, University of California, San Francisco, San Francisco, United States
ORCID iD: 0000-0002-8938-9889

**Abigail Buchwalter**
Cardiovascular Research Institute, University of California, San Francisco, San Francisco, United States, Department of Physiology, University of California, San Francisco, San Francisco, United States
ORCID iD: 0000-0001-7181-6961

**For correspondence:** abigail.buchwalter@ucsf.edu

## Editors



**Reviewer #1 (Public review):**

Summary:

The authors revisit the specific domains/signals required for redirection of an inner nuclear membrane protein, emerin, to the secretory pathway. They find that epitope tagging influences protein fate, serving as a cautionary tale for how different visualisation methods are used. Multiple tags and lines of evidence are used, providing solid evidence for the altered fate of different constructs.

Strengths:

This is a thorough dissection of domains and properties that confer INM retention vs secretion to the PM/lysosome, and will serve the community well as a caution regarding placement of tags and how this influences protein fate.

Weaknesses:

The specific biogenesis pathway for C-terminally tagged emerin might confound some interpretations. Appending the large GFP to the C-terminus may direct the fusion protein to a different ER insertion pathway than that used by the endogenous protein. How this might influence the fate of the tagged protein remains to be determined. In some ways this is beyond the scope of the current study, but should serve as a warning to epitope-tagging approaches.

https://doi.org/10.7554/eLife.105937.2.sa2

**Reviewer #2 (Public review):**

In this manuscript, Mella et al. investigate the effect of GFP tagging on the localization and stability of the nuclear-localized tail-anchored (TA) protein Emerin. A previous study from this group demonstrated that C-terminally GFP-tagged Emerin traffics to the plasma membrane and is eventually targeted to lysosomes for degradation. It has been suggested that the C-terminal tagging of TA proteins may shift their insertion from the post-translational TRC/GET pathway to the co-translational SRP-mediated pathway. Consistent with this, the

authors confirm that C-terminal GFP tagging causes Emerin to mislocalize to the plasma membrane and subsequently to lysosomes.

In this study, they investigate the mechanism underlying this misrouting. By manipulating the cytosolic domain and the hydrophobicity of the transmembrane domain (TMD), the authors show that an ER retention sequence and increased TMD hydrophobicity contribute to Emerin's trafficking through the secretory pathway.

This reviewer had previously raised the concern that the potential role of the GFP tag within the ER lumen in promoting secretory trafficking was not addressed. In the revised manuscript, the authors respond to this concern by examining the co-localization of Emerin-GFP with the ER exit site marker Sec31A. Their data show that the presence of the C-terminal GFP tag increases Emerin's propensity to engage ER exit sites, supporting the conclusion that GFP tagging promotes its entry into the secretory pathway.

https://doi.org/10.7554/eLife.105937.2.sa1

**Author Response:**

The following is the authors' response to the original reviews.

> ***Reviewer #1 (Public review):***
>
> *Summary:*
>
> *The authors revisit the specific domains/signals required for the redirection of an inner nuclear membrane protein, emerin, to the secretory pathway. They find that epitope tagging influences protein fate, serving as a cautionary tale for how different visualisation methods are used. Multiple tags and lines of evidence are used, providing solid evidence for the altered fate of different constructs.*
>
> *Strengths:*
>
> *This is a thorough dissection of domains and properties that confer INM retention vs secretion to the PM/lysosome, and will serve the community well as a caution regarding the placement of tags and how this influences protein fate.*
>
> *Weaknesses:*
>
> *Biogenesis pathways are not explored experimentally: it would be interesting to know if the lysosomal pool arrives there via the secretory pathway (eg by engineering a glycosylation site into the lumenal domain) or by autophagy, where failed insertion products may accumulate in the cytoplasm and be degraded directly from cytoplasmic inclusions.*

This manuscript is a Research Advance that follows previous work that we published in eLife on this topic (Buchwalter et al., *eLife* 2019; PMID 31599721). In that prior publication, we showed that emerin-GFP arrives at the lysosome by secretion and exposure at the PM, followed by internalization. While we state these previous findings in this manuscript, we did not explicitly restate here how we came to that conclusion. In the 2019 study, we (i) engineered in a glycosylation site, which demonstrated that emerin-GFP receives complex, Endo H-resistant N-glycans, indicating passage through the Golgi; (ii) performed cell surface labeling, which confirmed that emerin accesses the PM; and interfered with (iii) the early secretory pathway using brefeldin A and with (iv) lysosomal function using bafilomycin A1. Further, we ruled out autophagy as a major contributor to emerin trafficking by treating cells with the PI3K inhibitor KU55933, which had no effect on emerin's lysosomal delivery.

> *It would be helpful if the topology of constructs could be directly demonstrated by pulse-labelling and protease protection. It's possible that there are mixed pools of both topologies that might complicate interpretation.*

We demonstrate that emerin's TMD inserts in a tail-anchored orientation (C terminus in ER lumen) by appending a GFP tag to either the N or C terminus, followed by anti-GFP antibody labeling of unpermeabilized cells (Fig. 1G). This shows the preferred topology of emerin's wild type TMD.

As the reviewer points out, it is possible that our manipulations of the TMD sequence (Fig. 2D-E) alter its preferred topology of membrane insertion. We addressed this question by performing anti-GFP and anti-emerin antibody labeling of the less hydrophobic TMD mutant (EMD-TMDm-GFP) after selective permeabilization of the plasma membrane (Figure 2 supplement, panel F). If emerin biogenesis is normal, the GFP tag should face the ER lumen while the emerin antibody epitope should be cytosolic. If the fidelity of emerin's membrane insertion is impaired, the GFP tag could be exposed to the cytosol (flipped orientation), which would be detected by anti-GFP labeling upon plasma membrane permeabilization. We find that the C-terminal GFP tag is completely inaccessible to antibody when the PM is selectively permeabilized with digitonin, but is readily detected when all intracellular membranes are permeabilized with Triton-X-100. These data confirm that mutating emerin's TMD does not disrupt the protein's membrane topology.

> ***Reviewer #2 (Public review):***
>
> *In this manuscript, Mella et al. investigate the effect of GFP tagging on the localization and stability of the nuclear-localized tail-anchored (TA) protein Emerin. A previous study from this group showed that C-terminally GFP-tagged Emerin protein traffics to the plasma membrane and reaches lysosomes for degradation. It is suggested that the C-terminal tagging of tail-anchored proteins shifts their insertion from the post-translational TRC/GET pathway to the co-translational SRP-mediated pathway. The authors of this paper found that C-terminal GFP tagging causes Emerin to localize to the plasma membrane and eventually reach lysosomes. They investigated the mechanism by which Emerin-GFP moves to the secretory pathway. By manipulating the cytosolic domain and the hydrophobicity of the transmembrane domain (TMD), the authors identify that an ER retention sequence and strong TMD hydrophobicity contribute to Emerin trafficking to the secretory pathway. Overall, the data are solid, and the knowledge will be useful to the field. However, the authors do not fully answer the question of why C-terminally GFP-tagged Emerin moves to the secretory pathway. Importantly, the authors did not consider the possible roles of GFP in the ER lumen influencing Emerin trafficking to the secretory pathway.*
>
> ***Reviewer #2 (Recommendations for the authors):***
>
> *Major concerns:*
>
> *(1) The authors suggest that an ER retention sequence and high hydrophobicity of Emerin TMD contribute to its trafficking to the secretory pathway. However, these two features are also present in WT Emerin, which correctly localizes to the inner nuclear membrane. Additionally, the authors show that the ER retention sequence is normally obscured by the LEM domain. The key difference between WT Emerin and Emerin-GFP is the presence of GFP in the ER lumen. The authors missed investigating the role of GFP in the ER lumen in influencing Emerin trafficking to the secretory pathway. It is likely that COPII carrier vesicles capture GFP protein in the lumen as part of the bulk flow mechanism for transport to the Golgi compartment. The authors could easily test this by*

> *appending a KDEL sequence to the C-terminus of GFP; this should now redirect the protein to the nucleus.*

We agree with the reviewer's point that the presence of lumenal GFP somehow promotes secretion of emerin from the ER, likely at the stage of enhancing its packaging into COPII vesicles. We struggle to think about how to interpret the KDEL tagging experiment that the reviewer proposes, as the KDEL receptor predominantly recycles soluble proteins from the Golgi to the ER, while emerin is a membrane protein; and we have shown that emerin already contains a putative COPI-interacting RRR recycling motif in its cytosolic domain.

Nevertheless, we agree with the reviewer that it is worthwhile to test the possibility that addition of GFP to emerin's C-terminus promotes capture by COPII vesicles. We have evaluated this question by performing temperature block experiments to cause cargo accumulation within stalled COPII-coated ER exit sites, then comparing the propensity of various untagged and tagged emerin variants to enrich in ER exit sites as judged by colocalization with the COPII subunit Sec31a. These data now appear in Figure 4 supplement 1. These experiments indicate that emerin-GFP samples ER exit sites significantly more than does untagged emerin. Further, the ER exit site enrichment of emerin-GFP is dampened by shortening emerin's TMD. We do not see further enrichment of any emerin variant in ER exit sites when COPII vesicle budding is stalled by low temperature incubation, implying that emerin lacks any positive sorting signals that direct its selective enrichment in COPII vesicles. Altogether, these data indicate that both emerin's long and hydrophobic TMD and the addition of a lumenal GFP tag increase emerin's propensity to sample ER exit sites and undergo non-selective, "bulk flow" ER export.

> *(2) The authors nicely demonstrate that the hydrophobicity of Emerin TMD plays a role in its secretory trafficking. I wonder if this feature may be beneficial for cells to degrade newly synthesized Emerin via the lysosomal pathway during mitosis, as the nuclear envelope breakdown may prevent the correct localization of newly synthesized Emerin. The authors could test Emerin localization during mitosis. Such findings could add to the physiological significance of their findings. At the minimum, they should discuss this possibility.*

We thank the reviewer for this insightful suggestion. It is attractive to speculate that secretory trafficking might enable lysosomal degradation of emerin during mitosis, when its lamin anchor has been depolymerized. However, we think it is unlikely that mitotic trafficking contributes significantly to the turnover flux of untagged emerin; if it did, we would expect to see higher steady state levels and/or slowed turnover of emerin mutants that cannot traffic to the lysosome. We did not observe this outcome. Instead, mutations that enhance (RA) or impair (TMDm) emerin trafficking had no effect on the untagged protein's steady-state levels (Fig. 4G).

> *Minor concerns:*
>
> *(1) On page 7, the authors note that "FLAG-RA construct was not poorly expressed relative to WR, in contrast with RA-GFP (Figures S3C, 2I)." The expression levels of these proteins cannot be compared across two different blots.*

We apologize for this confusion; we were implying two distinct comparisons to internal controls present on each blot. We have adjusted the text to read "FLAG-RA construct was not poorly expressed relative to FLAG-WT (Fig. S3C) in contrast to RA-GFP compared to WT-GFP (Fig. 2I)."

> *(2) In the first paragraph of the discussion, the authors suggest that aromatic amino acids facilitate trafficking to lysosomes. However, they only replaced aromatic amino*

> *acids with alanine residues. If they want to make this claim, they should test other amino acids, particularly hydrophobic amino acids such as leucine.*

The reviewer may be inferring more import from our statement than we intended. We focused on these aromatic residues within the TMD because they contribute strongly to its overall hydrophobicity. Experimentally, we determined that nonconservative alanine substitutions of these aromatic residues inhibited trafficking. We do not state and do not intend to imply that the aromatic character of these residues specifically influences trafficking propensity, and we agree with the reviewer that to test such a question would require additional substitutions with non-aromatic hydrophobic amino acids.

We realize that our phrasing may have been misleading by opening with discussion of the aromatic amino acids; in the revised discussion paragraph, we instead lead with discussion of TMD hydrophobicity, and then state how the specific substitutions we made affect trafficking.

> *Reviewing Editor comments:*
>
> *While reviewer 1 did not provide any recommendations to the authors, I agree with this reviewer that the authors should validate the topology of their tagged proteins (at least for the one used to draw key conclusions). Given that Emerin is a tail-anchored protein, having a big GFP tag at the C-terminus could mess up ER insertion, causing the protein to take a wrong topology or even be mislocalized in the cytosol, particularly under overexpression conditions. In either case, it can be subject to quality control-dependent clearance via either autophagy, ERphagy, or ER-to-lysosome trafficking. I think that the authors should try a few straightforward experiments such as brefeldin A treatment or dominant negative Sar1 expression to test whether blocking conventional ER-to-Golgi trafficking affects lysosomal delivery of Emerin. I also think that the authors should discuss their findings in the context of the RESET pathway reported previously (PMID: 25083867). The ER stress-dependent trafficking of tagged Emerin to the PM and lysosomes appears to follow a similar trafficking pattern as RESET, although the authors did not demonstrate that Emerin traffic to lysosomes via the PM. In this regard, they should tone down their conclusion and discuss their findings in the context of the RESET pathway, which could serve as a model for their substrate.*

We agree that validating the topology of TMD mutants is important, and now include these experiments in the revised manuscript (please see our response to Reviewer 1 above).

Please see our response to Reviewer 1's public review; we previously determined that emerin-GFP undergoes ER-to-Golgi trafficking (see our 2019 study).

We recognize the major parallels between our findings and the RESET pathway. In our 2019 study, we found that similarly to other RESET cargoes, emerin-GFP travels through the secretory pathway, is exposed at the PM, and is then internalized and delivered to lysosomes. We discussed these strong parallels to RESET in our 2019 study. In this revised manuscript, we now also point out the parallels between emerin trafficking and RESET and cite the 2014 study by Satpute-Krishnan and colleagues (PMID 25083867)

https://doi.org/10.7554/eLife.105937.2.sa0